Influence of Numerical Dissipation on Computational Euler Equations for Vortex-Dominated Flows

Osama A. Kandil* and Andrew H. Chuang†
Old Dominion University, Norfolk, Virginia

Steady, supersonic vortex-dominated flows are solved using the unsteady Euler equations for conical flows around sharp- and round-edged delta wings. A finite-volume scheme with a four-stage Runge-Kutta time stepping and explicit second- and fourth-order dissipation terms has been developed to obtain the steady flow solution through psuedo time stepping. The grid is generated by using a modified Joukowski transformation. The scheme has been applied to flat-plate and elliptic-section delta wings at different angles of attack, freestream Mach numbers, and grid sizes. For the sharp-edged wings, separated-flow solutions are always obtained, while for round-edged wings both separated- and attached-flow solutions can be obtained, depending on the level of numerical dissipation. The round-edged results also show that the solutions are independent of the way time stepping is done—local time stepping and global minimum time stepping produce the same solutions.

Introduction

IN the early '60s, Stanbrook and Squire[1] classified the flowfield about sharp-edged delta wings according to the normal angle of attack and normal Mach number, α_N and M_N, into two main types: a flow with leading-edge separation and a flow with an attached flow at the leading edge. In Fig. 1a, the former type of flow is referred to as region A, and the latter type of flow is referred to as regions B and C. In region A, the flow separates at the leading edge (primary separation) and rolls up into a leading-edge vortex core that creates a suction-pressure peak on the wing upper surface with an adverse spanwise pressure gradient. The outboard, spanwise, boundary-layer flow on the upper surface separates due to the adverse spanwise pressure gradient forming a secondary separation and causing, for laminar boundary-layer flows, another suction peak in the spanwise pressure distribution. Depending on the flow conditions, tertiary separation may develop on the outboard side of the secondary point of separation.

In regions B and C, a detached or attached bow shock is formed upstream of the leading edge, the flow is attached at the leading edge, and supersonic flow expansions occur ending with an inboard conical shock. Depending on the shock strength, shock-induced separation may develop on the inboard side of the shock.

The Stanbrook-Squire diagram was modified by Vorropoulos and Wendt,[2] who introduced subregion A_1 within region A, where a conical shock was observed on the suction side under the leading-edge vortex. The flow in this region, between the wing surface and the lower surface of the leading-edge vortex, is analogous to the flow in a convergent-divergent channel where the accelerated supersonic flow ends with a shock.

Miller and Wood[3] expanded the Stanbrook-Squire diagram through an extensive experimental research program. Depending on M_N and α_N, they classified the flow into seven regions, as shown in Fig. 1b. In addition to the flows described, leading-edge separations with shock waves above the leading-edge vortex are also possible flows for subsonic and supersonic M_N at large α_N.

It is obvious that we are dealing with a very complex flowfield, which may include a leading-edge separation with a secondary separation, an attached leading-edge flow with an inboard shock and a possible shock-induced separation, or a combination of the leading-edge separation and the inboard shock with secondary and shock-induced separations. The complexity of the flowfield increases at large angles of attack when the leading-edge vortex core breaks down over the wing. The ultimate complexity of the flowfield is encountered during maneuverability, when the flowfield will change from one region to the other along with the effects of time history of the the flow.

In the computational area, a substantial volume of research work has recently been and is still being produced by several investigators to accurately predict certain types of the many complex types of flowfields presented previously. These prediction techniques are based on the full potential equation,[4-6] the Euler equations,[7-18] and the Navier-Stokes equations.[19-21] An extensive review of the physical aspects and numerical simulation of vortical flows is given by Newsome and Kandil.[22]

The study of vortex-dominated flow through the solution of steady, supersonic vortex-dominated flows, which are exact conical flows for the Euler equations, is a computationally economic approach that provides rich information on the computational schemes and their reliability for this type of flow in three-dimensional problems. Solutions for supersonic conical flows have recently been presented for sharp-edged[11-15] and round-edged[14-16] leading-edge delta wings. Using the central-difference finite-volume scheme with Runge-Kutta time stepping[11-13] or McCormack's unsplit, explicit, finite-difference scheme[14,15] for sharp-edged wings, separated-flow solutions have always been obtained independent of the grid fineness. On the other hand, the computational solutions of the upwind finite-volume scheme with flux splitting[15] for sharp-edged wings have shown attached flows with coarse grids and separated flows with fine grids.

For round-edged wings, McCormack's unsplit, explicit scheme produces separated-flow solutions with coarse grids and attached-flow solutions with fine grids.[14,15] On the other hand, the upwind finite-volume flux-splitting scheme[15] always

Received May 20, 1986; revision received March 9, 1987.

*Professor, Department of Mechanical Engineering and Mechanics. Member AIAA.

†Research Assistant, Department of Mechanical Engineering and Mechanics. Member AIAA.

produces attached-flow solutions irrespective of the grid fineness. In Ref. 16, and for the same round-edged wing used in Refs. 14 and 15, it has been shown that a very coarse grid using an upwind TVD scheme produces separated- and attached-flow solutions depending on the time stepping. It has been shown that with local time stepping, separated-flow solutions are obtained, while with global minimum time stepping, attached flow solutions are obtained. In Ref. 17, the authors have initially shown, using a central-difference finite-volume scheme with Runge-Kutta time stepping, that the inconsistent solutions for round-edged wings are strongly dependent on numerical dissipation.

In this paper, we investigate the influence of numerical dissipation on the solution obtained using the central-difference finite-volume scheme with Runge-Kutta time stepping for vortex-dominated flows. This includes sharp- and round-edged delta wings using coarse and fine grids. Keeping the dissipation level and the grid size fixed, we investigate the effect of time stepping, using local time stepping and global minimum time stepping, on the type of solution obtained. Additional results are given by the authors in Ref. 18.

Formulation and Computational Method

The conservation form of Euler equations for three-dimensional, unsteady compressible flow without external heat addition is

$$\frac{\partial \bar{q}}{\partial t}+\frac{\partial \bar{E}}{\partial x}+\frac{\partial \bar{F}}{\partial y}+\frac{\partial \bar{G}}{\partial z}=0 \tag{1}$$

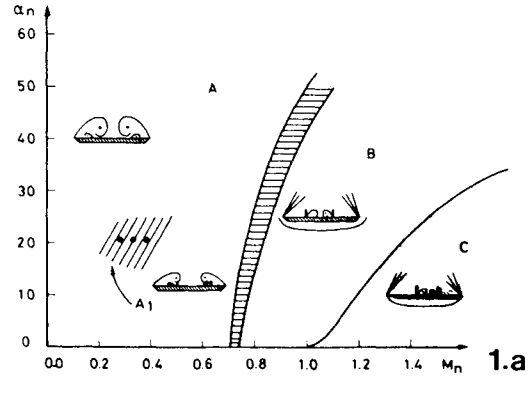

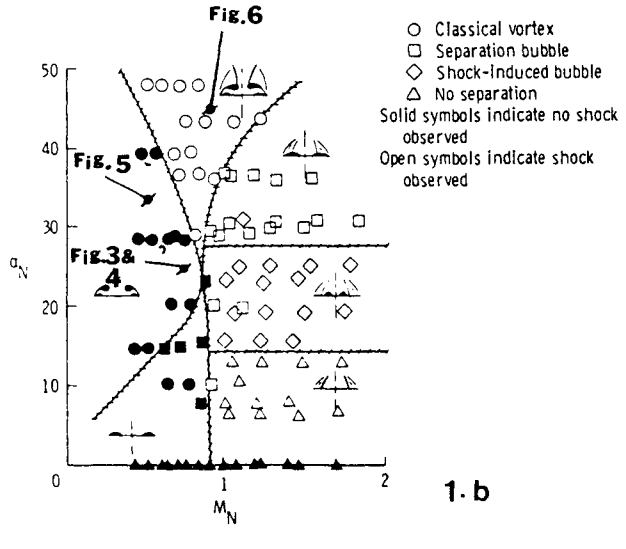

Fig. 1 Classification diagrams for delta wings; a) Stanbrook-Squire diagram with subregion A_1 (Ref. 2), b) Miller-Wood diagram (Ref. 3).

where the flow vector field $\bar{q}$ and the fluxes $\bar{E}$, $\bar{F}$, and $\bar{G}$ are given by

$$\bar{q}=[\rho,\rho u,\rho v,\rho w,\rho e]^t$$

$$\bar{E}=[\rho u,\rho u^2+p,\rho uv,\rho uw,\rho uh]^t$$

$$\bar{F}=[\rho v,\rho uv,\rho v^2+p,\rho vw,\rho vh]^t$$

$$\bar{G}=[\rho w,\rho uw,\rho vw,\rho w^2+p,\rho wh]^t \tag{2}$$

where

$$e=p/\rho(\gamma-1)+(u^2+v^2+w^2)/2 \tag{3}$$

and

$$h=e+p/\rho \tag{4}$$

In Eqs. (1–4), ρ is the density; u, v, and w the velocity components, p the pressure; e and h the total energy and enthalpy per unit mass; and γ the gas index.

For steady supersonic flows, Eqs. (1) and (2) are simplified by assuming a conical flowfield. Introducing the conical coordinates defined by

$$\xi=x,\quad \eta=y/x,\quad \zeta=z/x \tag{5}$$

in Eq. (1), we obtain

$$x\frac{\partial \bar{q}}{\partial t}+\frac{\partial \tilde{F}}{\partial \eta}+\frac{\partial \tilde{G}}{\partial \zeta}+2E=0 \tag{6}$$

where

$$\tilde{F}=\bar{F}-\eta\bar{E}\quad\text{and}\quad \tilde{G}=\bar{G}-\zeta\bar{E} \tag{7}$$

The pseudo time-stepping technique yields, upon reaching a steady flow, self-similar conical solutions. Equation (6) is solved at $x=1$.

Equation (6) is transformed to the computational domain $Y=Y(\eta,\zeta)$ and $Z=Z(\eta,\zeta)$. Integrating the resulting equation over the Y–Z computational domain, applying the divergence theorem, and using the result for a typical cell, the resulting difference equation is given by ($\Delta Y=\Delta Z=1$)

$$\left(\frac{\partial \hat{q}}{\partial t}\right)_{j,k}(J^{-1})_{j,k}+\hat{F}_{j,k+\frac{1}{2}}-\hat{F}_{j,k-\frac{1}{2}}+\hat{G}_{j+\frac{1}{2},k}$$
$$-\hat{G}_{j-\frac{1}{2},k}+2\hat{E}_{j,k}(J^{-1})_{j,k}=0 \tag{8}$$

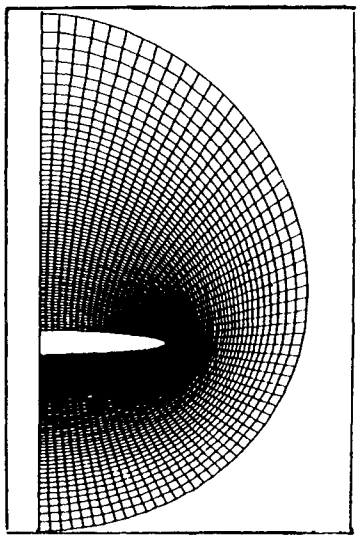

Fig. 2 Typical 64 × 64 coarse grid generated by a modified Joukowski transformation.

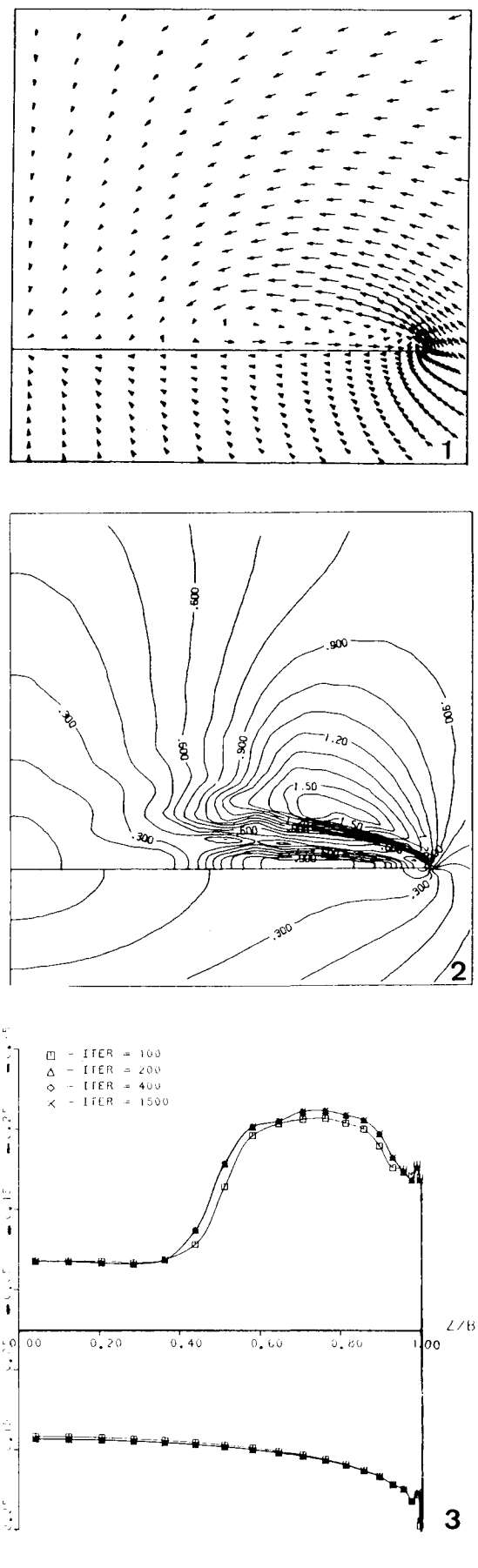

Fig. 3 Separated-flow solution, sharp edge, $M_\infty = 2$, $\alpha = 10$ deg, $\epsilon_2 = 0.1$, $\epsilon_4 = 0.001$; a) cross-flow velocity, b) cross-flow Mach contours, and c) surface pressure.

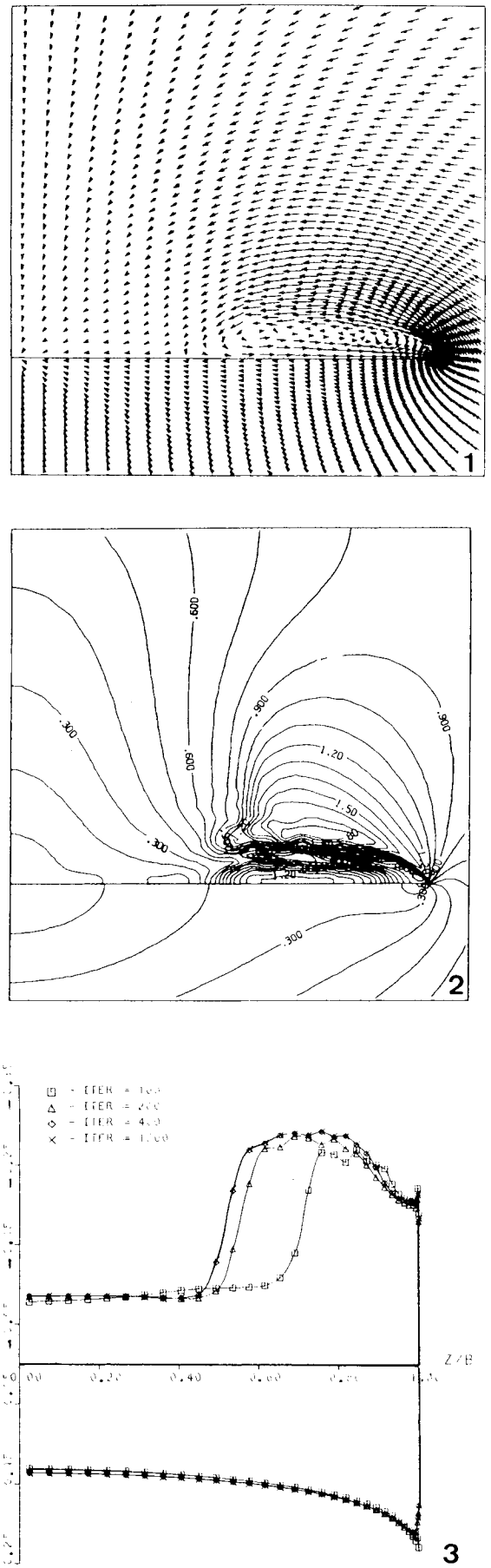

Fig. 4 Separated-flow solution, sharp edge, $M_\infty = 2$, $\alpha = 10$ deg, $\epsilon_2 = 0.1$, $\epsilon_4 = 0.001$; a) cross-flow velocity, b) cross-flow Mach contours, and c) surface pressure.

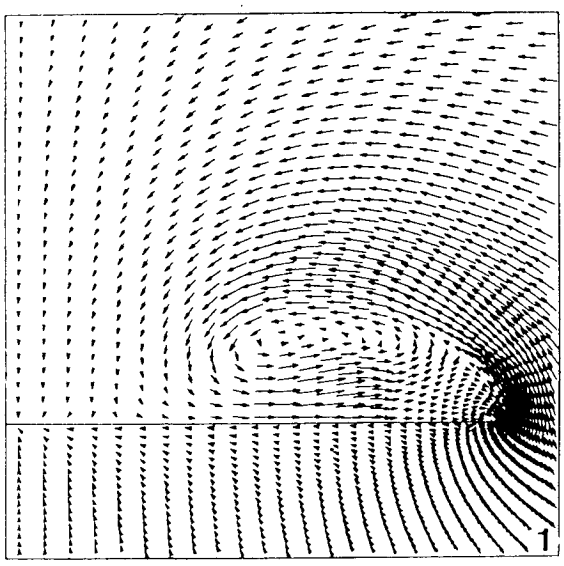

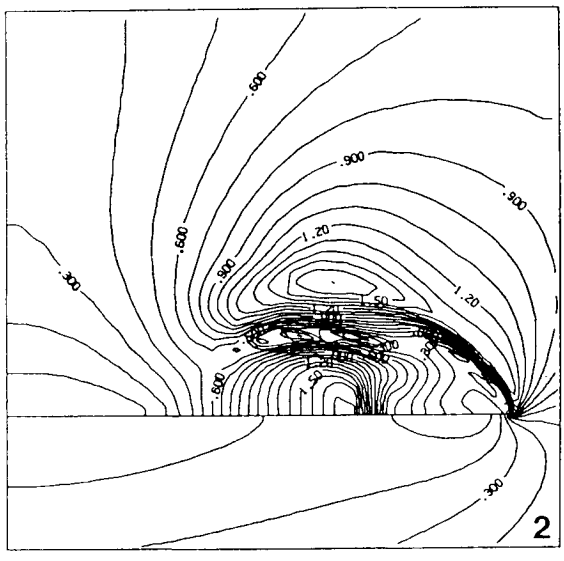

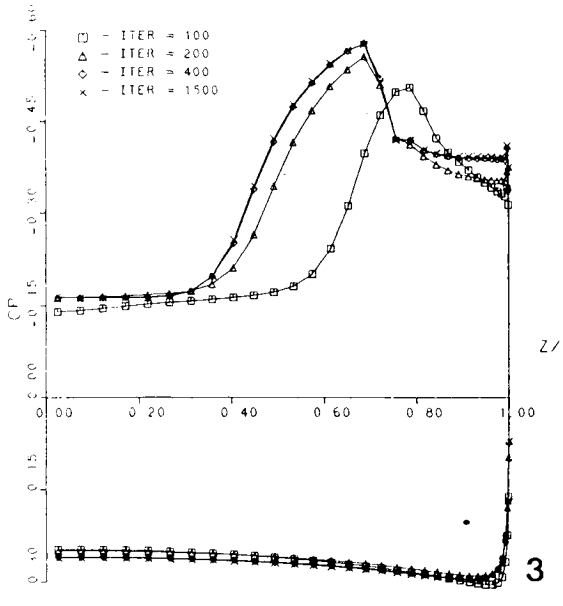

Fig. 5 Separated-flow solution, sharp edge, $M_\infty = 1.5$, $\alpha = 15$ deg, $\epsilon_2 = 0.12$, $\epsilon_4 = 0.0012$; a) cross-flow velocity, b) cross-flow Mach contours, and c) surface pressure.

where $\hat{q}$ and $\hat{F}$, $\hat{G}$, and $\hat{E}$ are the flow vector field and the flux components in the computational domain, respectively, and the half-integer subscript refers to the cell boundary. The inverse of the Jacobian is given by

$$J^{-1} = \eta_Y \zeta_Z - \eta_Z \zeta_Y \tag{9}$$

Second- and fourth-order dissipation terms[18] are added to Eq. (8), where the level of dissipation is changed through the change in the damping parameters ϵ_2 and ϵ_4.

The boundary conditions consist of a no-flux condition along the line of symmetry and on the wing surface, and a far-field boundary condition on the outer boundary of the computational domain. Along the line of symmetry, the pressure is extrapolated from the interior points, while on the wing the normal momentum equation is used to extrapolate the pressure from the interior points. The far-field condition is enforced by specifying freestream conditions on a large outer boundary such that the bow shock is captured as a part of the solution.

A modified Joukowski transformation[12] is used to generate the grid in the physical domain for the conical flow problems. The solutions are obtained by using four-stage, Runge-Kutta local time stepping starting from initial conditions corresponding to the freestream conditions, which represent an impulsive entry of the wing into the uniform flow. For time-accurate calculations, global minimum time stepping is used.

Computational Results

The conical flow code is applied to flat-plate and elliptic-section delta wings. The former represents the flow around a sharp leading edge, while the latter represents the flow around a round leading edge. The sweep-back angle β of all the computed cases is 70 deg. We used three grid sizes: a very coarse grid (28×38 cells), a coarse grid (64×64 cells), and a fine grid (100×100 cells), where the first number is the number of cells normal to the wing surface, $J_{\max}$, and the second number is the number of cells around the wing, $K_{\max}$. In all of the following examples, no Kutta or Kutta-like condition is enforced. Figure 2 shows a typical conical grid (64×64) generated by the modified Joukowski transformation.

Sharp-Edged Wings

Figures 3 and 4 show the results with a very coarse and a coarse grid, respectively, for a flat-plate delta wing. The damping parameters in the two cases are $\epsilon_2 = 0.1$ and $\epsilon_4 = 0.001$. In each figure, we show the cross-flow velocity, the cross-flow Mach contours, and the surface pressure at different iteration cycles. The cross-flow velocity, Figs. 3a and 4a, shows separated-flow solutions. The cross-flow Mach contour, Fig. 4b, indicates a small cross-flow shock existing under the vortex. The iteration history of the surface pressure shows that the flow fully separates either at the 100th iteration step, Fig. 3c, or at the 200th iteration step, Fig. 4c. By varying ϵ_2 between 0.1 and 0.01 and ϵ_4 between 0.004 and 0.001, separated-flow solutions have always been obtained. This case is indicated as Figs. 3 and 4 on the Miller-Wood diagram, Fig. 1b.

In Fig. 5, the results for a flat-plate sharp-edged delta wing with a grid size of 64×64 for $M_\infty = 1.5$ and $\alpha = 15$ deg are presented. The cross-flow velocity, Fig. 5a, shows the leading-edge vortex and two shocks; a weak shock above the vortex at its inner boundary and a strong shock below the vortex. The latter is analogous to the flow in a convergent-divergent channel flow. The cross-flow Mach contours, Fig. 5b, and the surface pressure, Fig. 5c, clearly show the strong shock formed under the vortex. These results confirm the observation by Vorropoulos and Wendt[2] and previous calculations using the integral equation approach.[6] This case is indicated as Fig. 5 on the Miller-Wood diagram, Fig. 1b.

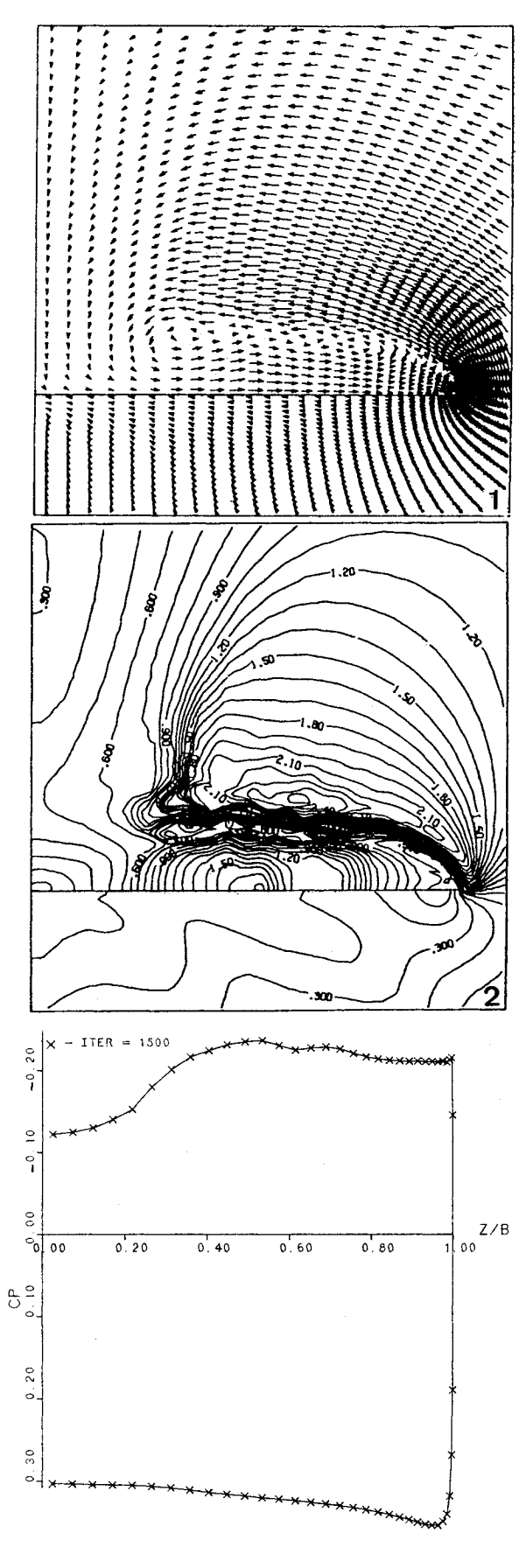

Fig. 6 Separated-flow solution, sharp edge, $M_\infty = 2.4$, $\alpha = 19$ deg, $\epsilon_2 = 0.1$, $\epsilon_4 = 0.001$; a) cross-flow velocity, b) cross-flow Mach contours, and c) surface pressure.

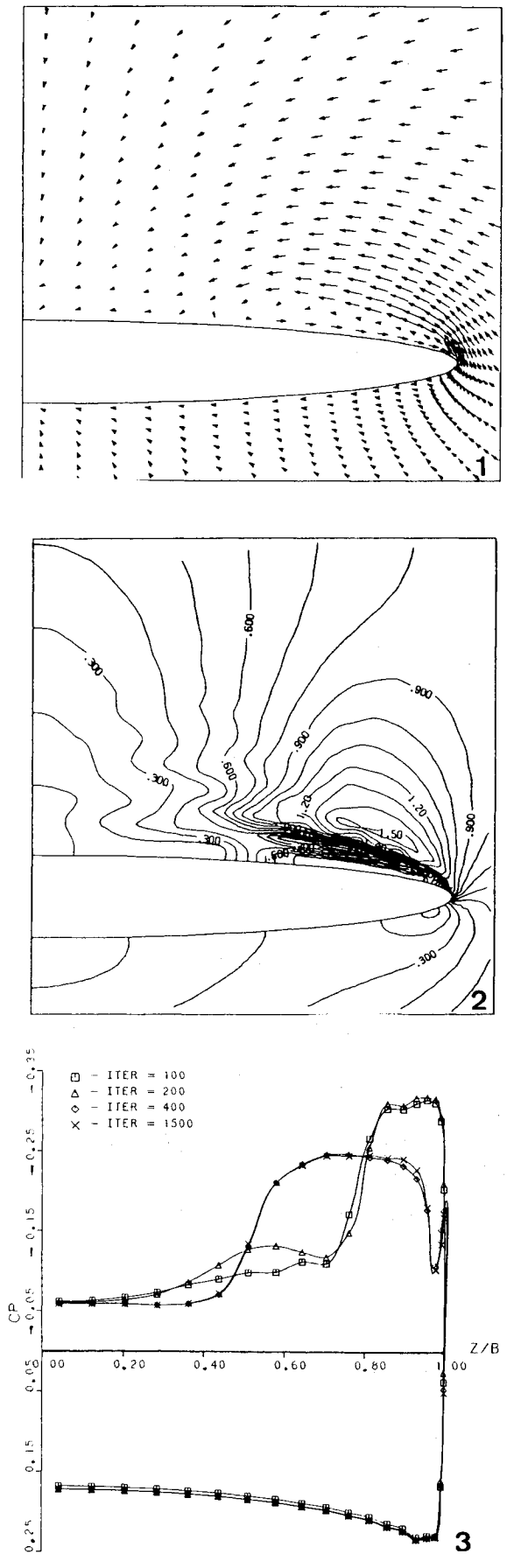

Fig. 7 High-dissipation-level solution, round edge, $M_\infty = 2$, $\alpha = 10$ deg, $\epsilon_2 = 0.25$, $\epsilon_4 = 0.004$; a) cross-flow velocity, b) cross-flow Mach contours, and c) surface pressure.

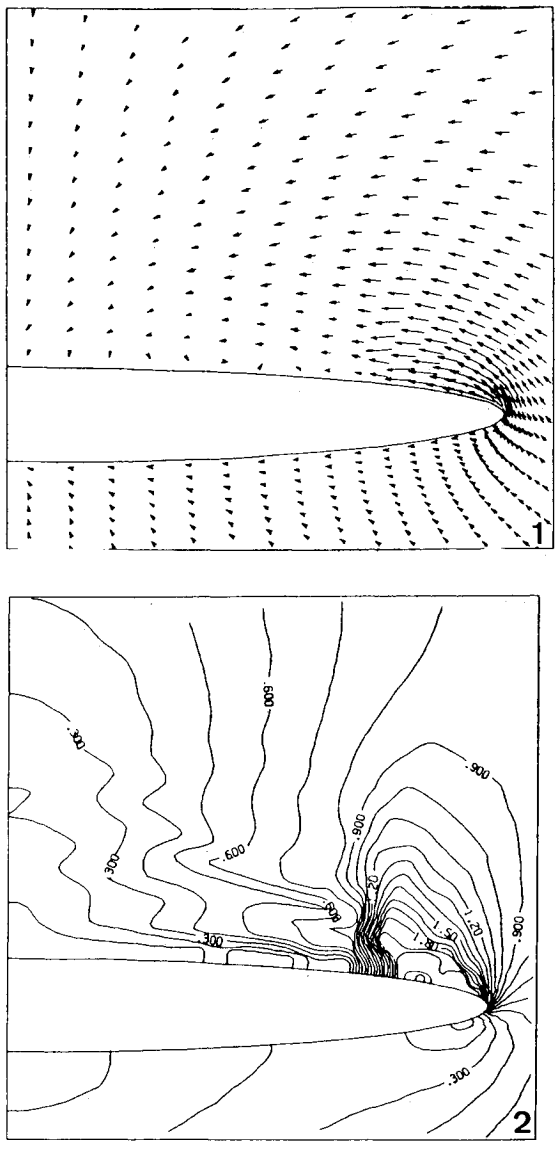

Fig. 8 Low-dissipation-level solution, round edge, $M_\infty = 2$, $\alpha = 10$ deg, $\epsilon_2 = 0.05$, $\epsilon_4 = 0.0008$; a) cross-flow velocity, b) cross-flow Mach contours, and c) surface pressure.

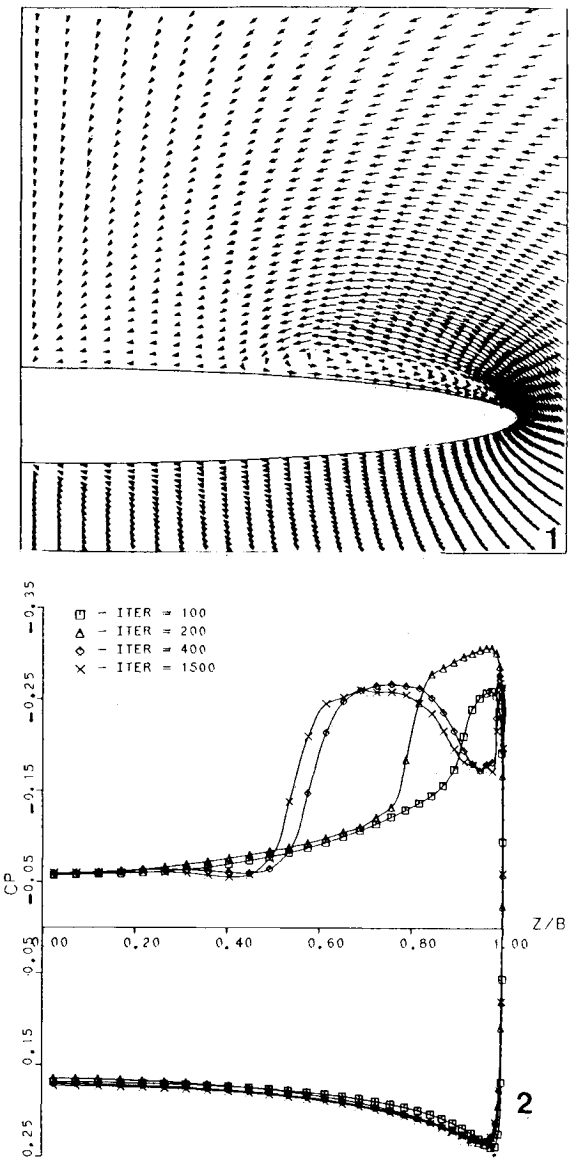

Fig. 9 High-dissipation-level solution, round edge, $M_\infty = 2$, $\alpha = 10$ deg, $\epsilon_2 = 0.25$, $\epsilon_4 = 0.004$; a) cross-flow velocity and b) surface pressure.

In Fig. 6, we show the results for a flat-plate sharp-edged delta wing with a grid size of 64×64 for $M_\infty = 2.4$ and $\alpha = 19$ deg. The results clearly show the leading-edge vortex and a strong shock above the vortex at its inner boundary. Note that the leading-edge vortex is flattened due to that shock. This case is indicated in Fig. 6 on the Miller-Wood diagram, Fig. 1b.

Since a Kutta condition has not been enforced, the smallest damping coefficients, as long as they are enough to dampen the oscillations, implicitly satisfy this condition. The dissipation terms act as real viscous terms in the Navier-Stokes equations where no Kutta condition is required. These results are in full agreement with those in Refs. 11–15.

The preceding solutions are good engineering solutions since they match the Navier-Stokes solutions for turbulent flows.

Round-Edged Wings

For all of the wings considered here, half the apex angle $\delta = 2$ deg and the sweep angle $\beta = 70$ deg. Figures 7 and 8 show the results for a very coarse grid with two sets of damping parameters ϵ_2 and ϵ_4 of (0.25, 0.004) and (0.05, 0.0008), respectively. The first level of dissipation causes

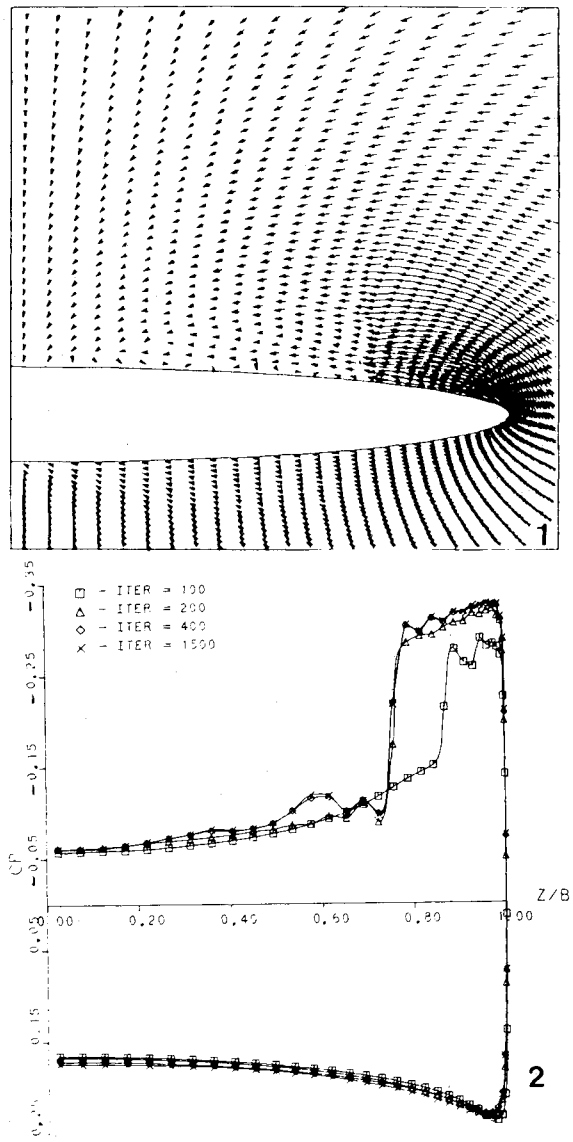

Fig. 10 Low-dissipation-level solution, round edge, $M_\infty = 2$, $\alpha = 10$ deg, $\epsilon_2 = 0.05$, $\epsilon_4 = 0.0008$; a) cross-flow velocity and b) surface pressure.

the flow to separate, Fig. 7, while the second level of dissipation does not, Fig. 8.

The separated-flow solution resembles the Navier-Stokes solution[14] and the real flow, and, hence, it is a good engineering solution, but it is not a proper Euler solution. It should be noted from the iteration history shown in Fig. 7c of the surface pressure that a cross-flow shock is formed at the 200th iteration step and the flow is attached at the leading edge. Behind the shock, there is a bump in the surface pressure corresponding to a small vortical flow. As the time stepping continues, the separated region at the shock base grows forming the primary vortex, and the shock disappears.

This type of solution is exactly the same as that obtained in Refs. 14 and 15 with a coarse grid (55×75) using McCormack's scheme (a central-differencing approximation) and in Ref. 16 with a very coarse grid (27×38) using the upwind biased TVD scheme with local time stepping.

Figure 8 shows an attached-flow solution with a cross-flow shock. It is noticed that some oscillations exist upstream and downstream of the shock due to the low level of dissipation. Although this solution is a proper Euler solution, it is not a good engineering solution.

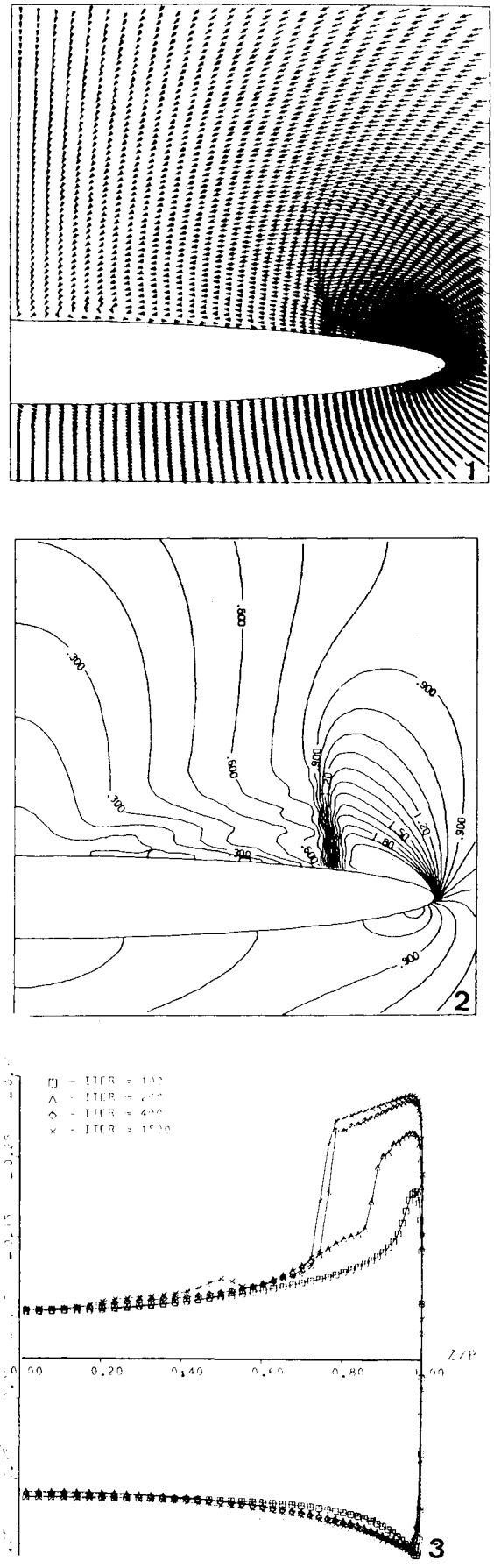

Fig. 11 Fine-grid solution, round edge, $M_\infty = 2$, $\alpha = 10$ deg, $\epsilon_2 = 0.25$, $\epsilon_4 = 0.04$; a) cross-flow velocity, b) cross-flow Mach contours, and c) surface pressure.

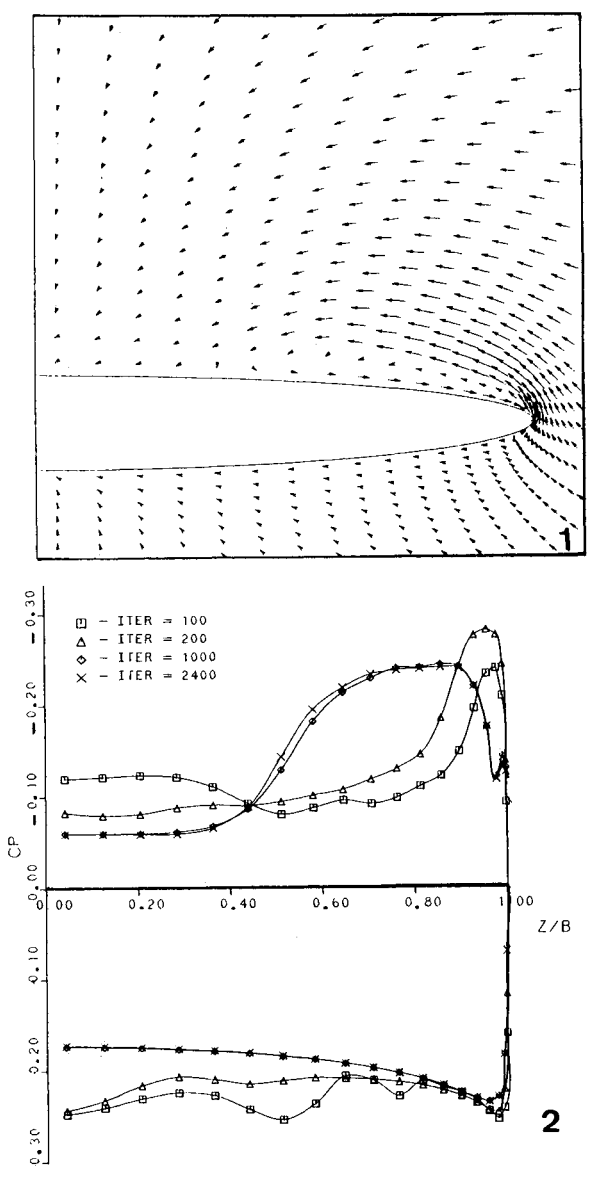

Fig. 12 Global-minimum time-stepping solution, round edge, $M_\infty = 2$, $\alpha = 10$ deg, $\epsilon_2 = 0.25$, $\epsilon_4 = 0.004$; a) cross-flow velocity and b) surface pressure.

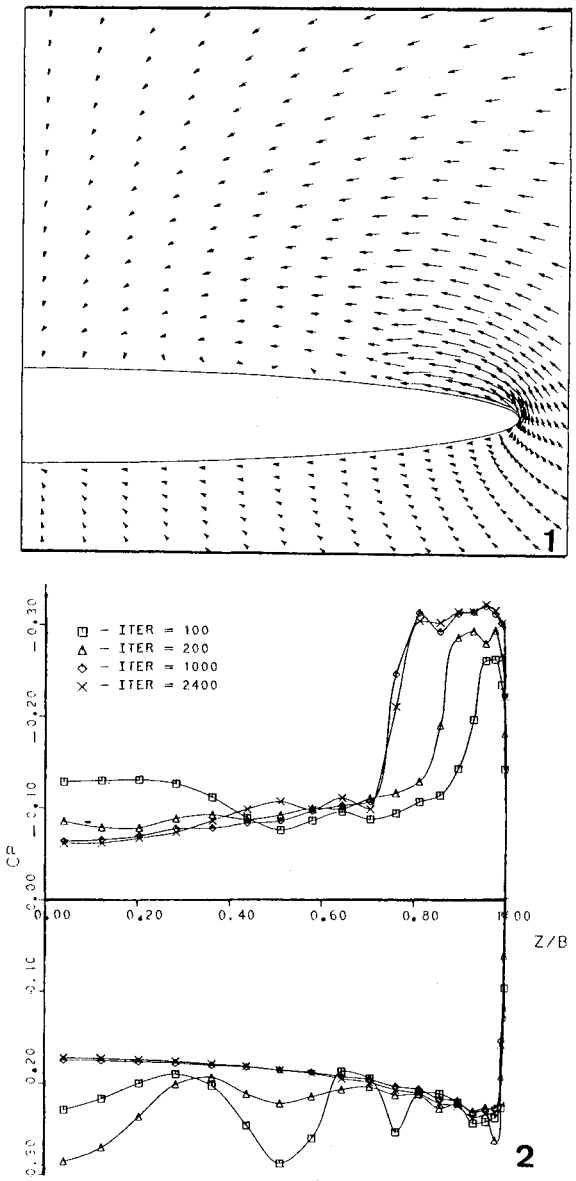

Fig. 13 Global-minimum time-stepping solution, round edge, $M_\infty = 2$, $\alpha = 10$ deg, $\epsilon_2 = 0.05$, $\epsilon_4 = 0.0008$; a) cross-flow velocity and b) surface pressure.

In Figs. 9 and 10, it is shown that the two types of solutions are still possible with the coarse grid and damping parameters of (0.25, 0.004) and (0.05, 0.0008). The iteration history given in Fig. 9b for the surface pressure shows clearly that an attached leading-edge flow with a cross-flow shock is produced in the first 200 iteration steps. Thereafter, flow separation and the formation of a primary vortex are produced. Figure 10 shows the results of the attached-flow solution with a cross-flow shock.

In Fig. 11, the results for a fine grid with a set of damping parameters of (0.25, 0.004) are presented. An attached-flow solution with a cross-flow shock is obtained. Here, no oscillations are evident around the shock. A small bump in the surface pressure (Fig. 11c) is noticed at the spanwise station of 0.5, which corresponds to a vortical region produced by the curved shock (numerical dissipation might have also contributed to this region), consistent with Crocco's theorem and Newsome's calculations[14] with the exception of its location.

Since the solutions obtained thus far are based on the local time stepping, because of its computational efficiency, and since Chakrvarthy and Ota[16] doubt that the separated-flow solution may be due to the local time stepping, the next point to be addressed is the effect of using global-minimum time stepping. Figures 12 and 13 show the results of this test for a very coarse grid with the same sets of damping parameters as used to obtain the separated- and attached-flow solutions (the same cases as those in Figs. 7 and 8). Figure 12 shows that global-minimum time stepping produces the same solution as that obtained with local time stepping—a separated flow with $\epsilon_2 = 0.25$ and $\epsilon_4 = 0.004$. Figure 13 shows again that global-minimum time stepping produces the same solution as that obtained with local time stepping—an attached flow with $\epsilon_2 = 0.05$ and $\epsilon_4 = 0.0008$. The conclusion is simple: For the same damping coefficients, local or global-minimum time stepping produces the same solution.

Concluding Remarks

The influence of dissipation terms on Euler equation solutions, for supersonic vortex-dominated flows about sharp- and round-edged delta wings, using a central-difference finite-volume method with Runge-Kutta time stepping and explicit second- and fourth-order dissipation terms have been presented. For flat-plate sharp-edged delta wings, we have shown that a separated-flow solution is obtained irrespective of the

values of damping terms (as long as they are enough to obtain a stable solution) or the grid sizes. Hence, these solutions are good engineering solutions. For elliptic-section round-edged delta wings, we have shown that separated- and attached-flow solutions, using very coarse and coarse grids, are possible, depending on the values of the damping parameters. We have also shown that the solution is independent of the way time stepping is done—local and global-minimum time stepping produce the same solutions. For round-edged wings, a proper Euler solution (attached flow at the leading edge) is obtained only with a fine grid. Such a solution is not a good engineering solution, and hence, the Navier-Stokes equation or a simplified form of it must be used to obtain proper equation, good engineering solutions.

References

[1]Stanbrook, A. and Squire, L.C., "Possible Types of Flow at Swept Leading Edges," *Aeronautical Quarterly*, Vol. XV, Feb. 1964.

[2]Vorropoulos, G. and Wendt, J.F., "Laser Velocimetry Study of Compressible Effects on the Flow Field of a Delta Wing," AGARD CP 342, April 1983.

[3]Miller, D.S. and Wood, R.W., "Lee-Side Flow Over Delta Wings at Supersonic Speeds," NASA TP 2430, 1985.

[4]Kandil, O.A., "Numerical Prediction of Vortex Cores from the Leading and Trailing Edges of Delta Wings," ICAS Paper 14.2, 12th Congress of the International Council of the Aeronautical Sciences, Munich, Federal Republic of Germany, Oct. 1980.

[5]Kandil, O.A., Chu, L.C., and Tureaud, T., "A Nonlinear Hybrid Vortex Method for Wings at Large Angle of Attack," *AIAA Journal*, Vol. 22, March 1984, pp. 329–336.

[6]Kandil, O.A. and Yates, E.C. Jr., "Computation of Transonic Vortex Flows Past Delta Wings—Integral Equation Approach," *AIAA Journal*, Vol. 24, Nov. 1986, pp. 1729–1736.

[7]Rizzi, A., Eriksson, L.E., Schmidt, W., and Hitzel, S.M., "Simulation Vortex Flows Around Wings," AGARD CP 342, April 1983, pp. 21.1–21.14.

[8]Raj, P. and Sikora, J.A., "Free-Vortex Flows: Recent Encounters with a Euler Code," AIAA Paper 84-0135, Jan. 1984.

[9]Rizzi, A., "Three-Dimensional Solutions to Euler Equations with One Million Grid Points," *AIAA Journal*, Vol. 23, Dec. 1985, pp. 1986–1987.

[10]Krause, E., Shi, X.G., and Hartwich, P.M., "Computation of Leading Edge Vortices," AIAA Paper 83-1907, July 1983.

[11]Powell, K., Murman, E., Perez, E., and Baron, J., "Total Pressure Loss in Vortical Solutions of the Conical Euler Equations," AIAA Paper 85-1701, July 1985.

[12]Murman, E., Powell, K., and Miller, D., "Comparison of Computations and Experimental Data for Leading Edge Vortices, Effects of Yaw and Vortex Flaps," AIAA Paper 86-0439, Jan. 1986.

[13]Murman, E.M. and Rizzi, A., "Applications of Euler Equations to Sharp Edge Delta Wings with Leading Edge Vortices," AGARD Symposium on Application of Computational Fluid Dynamics in Aeronautics, Aux-En-Provence, France, April 1986.

[14]Newsome, R.W., "A Comparison of Euler and Navier-Stokes Solutions for Supersonic Flow Over a Conical Delta Wing," *AIAA Journal*, Vol. 24, April 1986, pp. 552–561.

[15]Newsome, R.W. and Thomas, J.L., "Computation of Leading-Edge Vortex Flows," Vortex Flows Aerodynamics Conference, NASA CP-2416, Vol. 1, VA, Oct. 1985.

[16]Chakrvarthy, S.R. and Ota, D.K., "Numerical Issues in Computing Inviscid Supersonic Flow Over Concial Delta Wings," AIAA Paper 86-0440, Jan. 1986.

[17]Kandil, O.A. and Chuang, A., "Numerical Dissipation Effects in Finite-Volume Euler Solutions for Conical Vortex Dominated Flows," *Computational Mechanics—Theory and Applications*, Springer-Verlag, Tokyo, Japan, May 1986, pp. X1.57–X1.64.

[18]Kandil, O.A. and Chuang, A., "Influence of Numerical Dissipation in Computing Supersonic Vortex-Dominated Flow," AIAA Paper 86-1073, May 1986.

[19]Newsome, R.W. and Adams, M.S., "Numerical Simulation of Vortical-Flow Over an Elliptical-Body Missile at High Angles of Attack," AIAA Paper 86-0559, Jan. 1986.

[20]Rizetta, D.P. and Shang, J.S., "Numerical Simulation of Leading Edge Vortex Flows," *AIAA Journal*, Vol. 24, Feb. 1986, pp. 237–245.

[21]Thomas, J.L. and Newsome, R.W., "Navier-Stokes Computations of Lee-Side Flows Over Delta Wings," AIAA Paper 86-1049, May 1986.

[22]Newsome, R.W. and Kandil, O.A., "Vortical Flow Aerodynamics—Physical Aspects and Numerical Simulation," AIAA Paper 87-0205, Jan. 1987.